

Sponge-rich sediment recycling in a Paleozoic continental arc driven by mélangé melting

Huichuan Liu^{1,2*}, Sune G. Nielsen^{3,4*} and Guangyou Zhu⁵

¹State Key Laboratory of Petroleum Resources and Prospecting, China University of Petroleum (Beijing), Beijing 102249, China

²College of Geosciences, China University of Petroleum (Beijing), Beijing 102249, China

³NIRVANA Laboratories, Woods Hole Oceanographic Institution, Woods Hole, Massachusetts 02543, USA

⁴Department of Geology and Geophysics, Woods Hole Oceanographic Institution, Woods Hole, Massachusetts 02543, USA

⁵Research Institute of Petroleum Exploration and Development, PetroChina, Beijing 100083, China

ABSTRACT

Slab material transfer processes in continental arcs can be challenging to decipher because magmas are often characterized by significant contributions from continental material. In this study, we identified a Prototethyan continental arc (419–418 Ma) that is now located in the Dazhonghe area of the southeast Tibetan Plateau, which, based on Sr-Nd-Hf-O-Si isotope relationships, implies no detectable continental material contributions. The Dazhonghe arc rocks display much lower $\delta^{30}\text{Si}$ values than modern arc rocks and average mantle; this is best explained by subduction of sponge-rich marine sediments, which are thought to have been the dominant marine organisms during the Neoproterozoic and early Paleozoic. Our mixing calculations reveal that only bulk mixing among sponge-rich sediments, altered oceanic crust (AOC), and the depleted mantle would be capable of accounting for all the Sr-Nd-Hf-O-Si isotope compositions. This finding implies that the Dazhonghe arc magmas were generated by melting of a mélangé that formed at the slab-mantle interface. The Dazhonghe continental arc is the first for which mélangé melting has been confirmed.

INTRODUCTION

Continental arcs form above subduction zones where the upper plate is composed of thick continental lithosphere and exhibits much stronger geochemical affinities with continental crust than oceanic arcs (Kelemen and Behn, 2016) because continental material contributions, which are absent in oceanic arcs, play an important role in their generation. With ongoing arc magmatism, which can be as long as 500 m.y., such as in the Andes (Ducea et al., 2015), the overlying continental crust is continuously consumed. Theoretically, the late phase of continental arc magmatism could assimilate little or no continental crust material and record the most depleted radioactive isotope compositions. However, the geochemical compositions, source nature, and petrogenetic processes of a continental arc without continental crust contributions are still enigmatic.

Arc rocks are characterized by negative anomalies in high field strength elements (HFSEs; i.e., Nb, Ta, and Ti) on primitive mantle-normalized multi-element spider diagrams, which are generally attributed to partial melting of a mantle wedge metasomatized by marine sediment melts and/or altered oceanic crust (AOC) fluids (Fig. 1A; Ulmer and Trommsdorff, 1995). An alternative genetic model for global arc rocks proposes that partial melting of subducted mélangé can also explain such geochemical features (Bebout, 2007; Marschall and Schumacher, 2012; Nielsen and Marschall, 2017). In this model, sediments, AOC, and/or hydrated mantle physically mix to form hybrid mélangé rocks along the interface between the subducted slab and the overlying mantle (Fig. 1B). This mélangé subsequently rises into the mantle wedge, where it dehydrates and melts to form arc magmas. Ascertaining the model that characterizes continental arcs is still a pending problem because, to date, only oceanic arc data have been shown to conform

to the mélangé model (Nielsen and Marschall, 2017; Shu et al., 2022).

Radiogenic isotope ratios, such as Sr-Nd-Hf, together with trace-element ratios are effective in discriminating the mantle metasomatism and mélangé genetic models for arc rocks (Nielsen and Marschall, 2017), but they cannot unambiguously distinguish continental crust from AOC and marine sediment contributions in arc magmas. This renders it challenging to use such data to investigate slab material transfer in continental arcs. As a complement, the stable O and Si isotope compositions may theoretically be used to test the two genetic models because marine sediments display significantly fractionated Si and O isotope compositions relative to the mantle (Sutton et al., 2013; Stamm et al., 2020). In this study, we selected the Prototethyan continental andesite arcs in the SE Tibetan Plateau as the target (Figs. S1 and S2 in the Supplemental Material¹) and carried out elemental and Sr-Nd-Hf-Si-O isotope analyses to investigate their sources and their genetic mechanism.

PROTOTETHYAN SUTURE AND CONTINENTAL ARC BELT IN THE SE TIBETAN PLATEAU

A Prototethyan ocean developed during the late Neoproterozoic to early Paleozoic along the northern margin of eastern Gondwana in the southeastern Tibetan Plateau area (Wang et al., 2018). The southeast Tibetan Plateau is known as the Sanjiang (Three Rivers) tectonic zone in Chinese literature (Fig. S1B). Prototethyan oceanic crust relicts (i.e., Nantinghe ophiolites) and arc magmatic rocks occur along the Lancangjiang tectonic belt, which were then superimposed by Paleotethyan

*E-mails: lhc@cup.edu.cn; sn Nielsen@whoi.edu

¹Supplemental Material. Detailed analytical methods, Tables S1–S5, and Figures S1–S5. Please visit <https://doi.org/10.1130/G50395.1> to access the supplemental material and contact editing@geosociety.org with any questions.

CITATION: Liu, H., Nielsen, S.G., and Zhu, G., 2023, Sponge-rich sediment recycling in a Paleozoic continental arc driven by mélangé melting: *Geology*, v. 51, p. 75–79, <https://doi.org/10.1130/G50395.1>

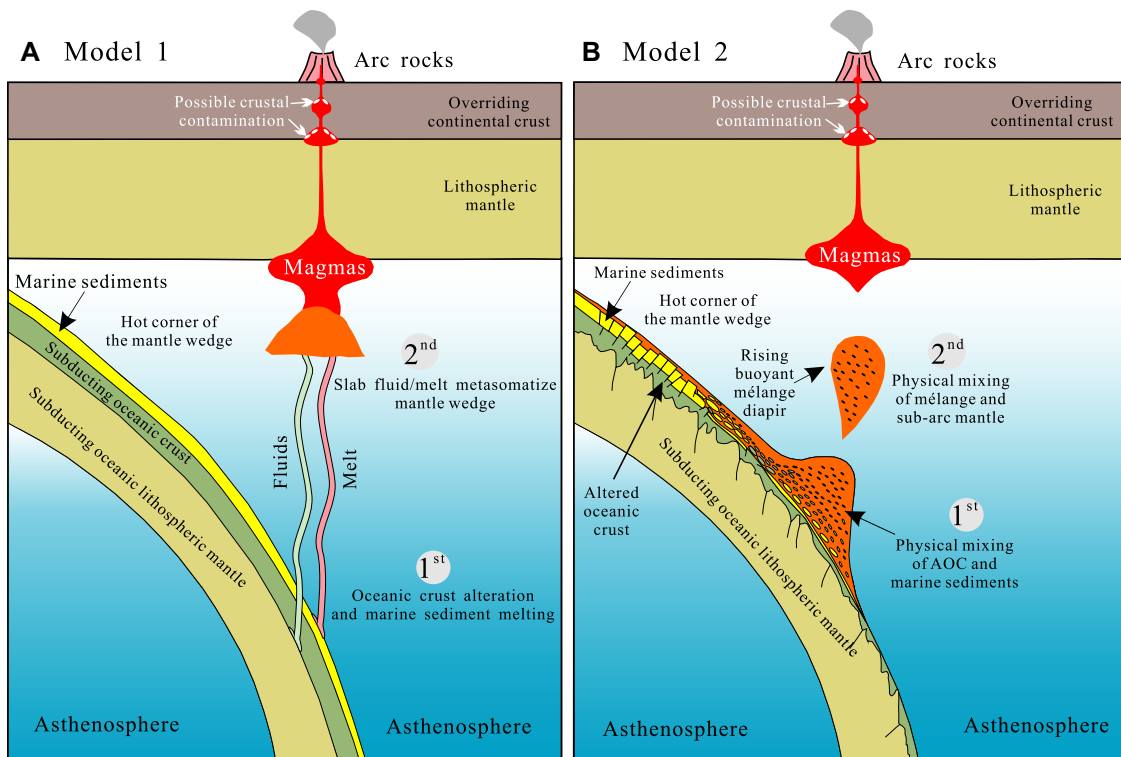


Figure 1. Illustration of two different end-member models of slab material transport in subduction zones (Nielsen and Marschall, 2017). (A) In the conventional model, sediment melts and fluids from altered oceanic crust (AOC) mix with ambient mantle melts to form arc magmas. (B) In the mélange model, sediments, AOC, and hydrated mantle physically mix to form hybrid mélange rocks.

ocean subduction and subsequent collision between the Sibumasu and Indochina blocks during the Triassic (Wang et al., 2018; Liu et al., 2019).

One of the most complete arc volcanic sequences in the southeastern Tibetan Plateau occurs in the Dazhonghe area, 30 km east of the Nantinghe ophiolites, and it consists of basaltic andesite, andesite, andesitic tuff, dacite, dacitic tuff, rhyolite, rhyolitic tuff, and tuffaceous sandstone with a total thickness of 3000 m (Fig. S2; Liu et al., 2019). These rocks show calc-alkaline arc-type elemental features, e.g., enrichments in large ion lithophile elements (LILEs) and depletions in HFSEs (Fig. S3). In tectonic discrimination diagrams, the Dazhonghe basalts and andesites ($\text{SiO}_2 < 63 \text{ wt}\%$) plot in the volcanic arc field, and the felsic rocks ($\text{SiO}_2 > 63 \text{ wt}\%$) plot in the volcanic arc granite field (Liu et al., 2019). Between the Dazhonghe arc and Nantinghe ophiolite, Neoproterozoic crustal materials (i.e., Lancang Group) crop out (Fig. S1B). Therefore, the Dazhonghe arc is a typical continental arc.

SAMPLING AND ANALYTICAL RESULTS

Zircon U-Pb ages and whole-rock element and Sr-Nd isotope data were reported previously (Liu et al., 2019), and the present study carried out *in situ* zircon Lu-Hf-O isotope and whole-rock Si isotope analyses on the Dazhonghe arc rocks. Analytical methods are described in the Supplemental Material and results are listed in Tables S1–S4 therein.

In Situ Zircon Lu-Hf-O Isotopes

Two samples were selected for Lu-Hf-O isotope analyses, with 14 and 13 individual zircon measurements, respectively. The stated errors for Hf isotope signatures refer to 2 standard error (SE). The mean O isotope values were $\delta^{18}\text{O} = +5.3\text{‰} \pm 0.3\text{‰}$ and $+5.5\text{‰} \pm 0.3\text{‰}$, and mean $\epsilon_{\text{Hf}}(t)$ values were $+14.8 \pm 2.9$ and $+14.3 \pm 2.9$, respectively (Fig. 2; Fig. S4). These high zircon $\epsilon_{\text{Hf}}(t)$ values are consistent with the corresponding whole-rock radiogenic Nd isotope compositions, which ranged from $\epsilon_{\text{Nd}}(t) = +5.5$ to $+4.9$ (Fig. 3; Liu et al., 2019). However, the melt O isotope compositions, recalculated from the zircon values using the equation [$\text{melt } \delta^{18}\text{O} \approx \text{zircon } \delta^{18}\text{O} + 0.0612 \times (\text{SiO}_2 \text{ wt}\%) - 2.5$] (Valley et al., 2005), exhibited values substantially higher than the mantle (Fig. 2A), indicating the presence of a crustal component in the Dazhonghe arc magmas.

Whole-Rock Si Isotope Results

The Dazhonghe volcanic samples displayed low $\delta^{30}\text{Si}$ values of -0.47‰ to -0.71‰ , which are much lighter than those of previously reported continental crust, island-arc basalt, mid-ocean ridge basalt (MORB), ocean-island basalt, and average mantle (Fig. 4; Savage et al., 2011, 2012; Pringle et al., 2016). Furthermore, fractional crystallization produces residual melts that are progressively enriched in the heavy Si isotopes (Savage et al., 2014), which is opposite to the observed low $\delta^{30}\text{Si}$ values (Fig. 4).

DISCUSSION

No Continental Crust Contribution

One sample studied here, 15YN-41G2, had low SiO_2 content (49.88 wt%) and high Mg# (61.80). Hence, the Dazhonghe volcanic rocks cannot have been derived exclusively from continental crust melting. Mantle-derived magmas in a continental arc are always likely to assimilate or be contaminated by crustal materials during their rise through the continental crust (Mackie et al., 2005). However, the following observations argue against significant continental material contributions to the generation of the Dazhonghe arc rocks:

(1) Significant crustal assimilation would produce unradiogenic Nd and Hf isotope values, which are not observed in the Dazhonghe arc rocks (Figs. 2 and 3). Our samples have high whole-rock $\epsilon_{\text{Nd}}(t)$ (mean value $+5.2$) and zircon $\epsilon_{\text{Hf}}(t)$ values (weighted average value $+14.6 \pm 2.9$), even higher than the contemporaneous depleted mantle-derived Nantinghe ophiolites ($\epsilon_{\text{Nd}}[t] = +1.9$, zircon $\epsilon_{\text{Hf}}[t] = +5.0$; Liu et al., 2019). Juvenile crust typically has more unradiogenic Nd and Hf isotope compositions than contemporaneous ophiolites, such as those found in the Nantinghe area, which implies that juvenile crust assimilation was likely very minor.

(2) The $\delta^{30}\text{Si}$ values (-0.47‰ to -0.71‰) are much lower than those previously reported for the continental crust (Savage et al., 2013). Crustal assimilation would only produce $\delta^{30}\text{Si}$ values lower than the mantle if S-type granites were added (Fig. 4A). However, the range

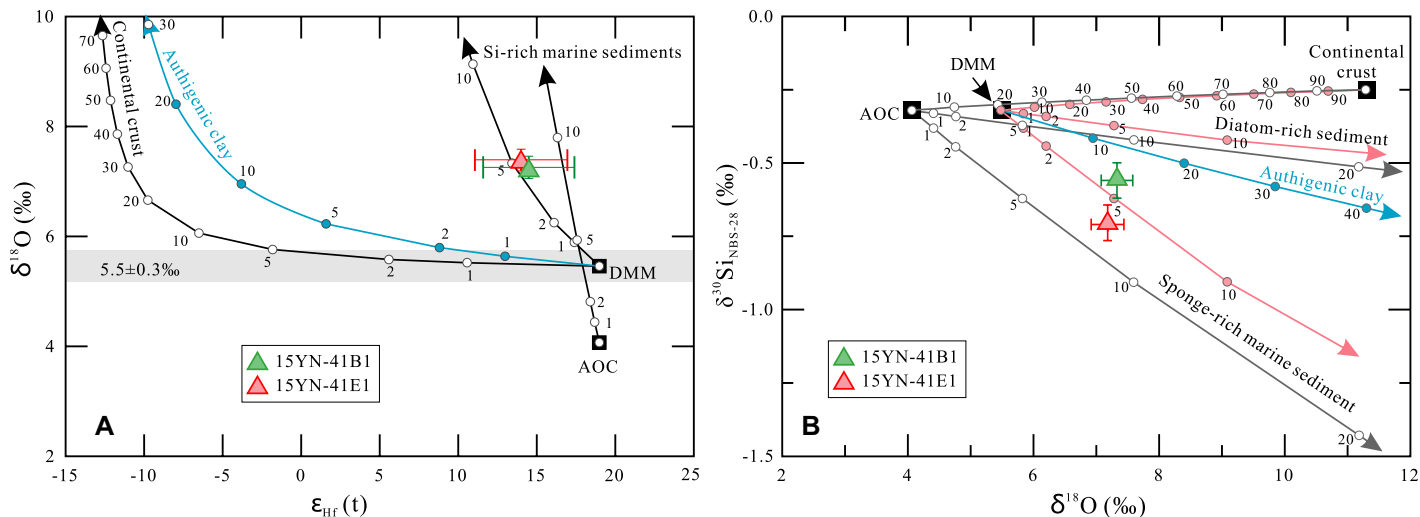


Figure 2. (A) Plots of melt $\epsilon_{\text{Hf}}(t)$ versus $\delta^{18}\text{O}$ and (B) $\delta^{18}\text{O}$ versus $\delta^{30}\text{Si}_{\text{NBS-28}}$ for Dazhonghe arc rocks. Values of mixing end members and associated references are listed in Table S5 (see footnote 1). AOC—altered oceanic crust; DMM—depleted mid-ocean-ridge basalt mantle.

of $\delta^{30}\text{Si}$ values in S-type granites is -0.11 to -0.41 , which does not overlap with our samples ($\delta^{30}\text{Si} = -0.47$ to -0.71).

(3) Crustal contamination, if any, might decrease the Nb/La ratios, resulting in a positive correlation between MgO and Nb/La ratios. No such correlations were observed in our samples (Liu et al., 2019).

(4) The addition of crustal materials to mafic magma produces plagioclase and pyroxene with resorbed cores and oscillatory zoning. No such plagioclase or pyroxene was found in the Dazhonghe volcanic rocks (Liu et al., 2019).

Mixed Source of Subducted Mélange and Depleted Mantle

Element and isotope fractionations are different for the mantle-wedge metasomatism and mélange melting models of mantle source enrichment in subduction zones, which enables us to test which model more accurately reproduces observed data in arc lavas (Nielsen and Marschall, 2017). Here, we used some of the same tests previously developed (Nielsen and Marschall, 2017) and further

used our new Si-O isotope data to perform additional tests.

Sr-Nd Isotope and Elemental Evidence

In the metasomatized mantle model with sediment melting and AOC and/or serpentinite dehydration, trace-element fractionation occurs within the slab, followed by mixing of these mobile components with the mantle wedge. In contrast, mélange models invoke physical mixing of the different bulk slab components first, followed by melting and dehydration processes that cause trace-element fractionation. Hence, the key to discriminating these two models is identifying the mixing end members: marine sediment and AOC, or sediment melts, AOC fluids, and subarc mantle (Fig. 1). Both sediment melts and AOC fluids display similar Sr-Nd isotope compositions and much lower Nd/Sr ratios than their respective bulk counterparts (marine sediment and AOC), and mixing curves between the mantle and these components in Sr-Nd isotope space have very different curvatures from those dominated by the mixing of bulk sediment (and bulk AOC) and the subarc mantle (Nielsen

and Marschall, 2017). We chose Sr and Nd partition coefficients of 7.3 and 0.35, respectively, following previous work (Hermann and Rubatto, 2009), and performed binary mixing calculations between depleted MORB mantle (DMM) and marine sediment and AOC, or sediment melts, respectively. The Dazhonghe samples plot between the DMM–marine sediment and DMM–AOC mixing lines, far away from the DMM–sediment melt mixing trajectories (Fig. 3A).

Both Hf and Nd show low mobility in hydrous fluids, so the Hf/Nd ratio of arc magmas may be the result of fractionation during either sediment or mélange melting, and their Nd isotope variations should primarily relate to mixing of the mantle with either sediment melts or bulk sediment (Nielsen and Marschall, 2017). Mixing between the mantle and bulk sediment or mixing between the mantle and sediment melts will follow different lines, as shown in Figure 3B. The Dazhonghe samples show limited variation in Nd isotopes and variable Hf/Nd ratios and fall along horizontal partial melting lines. The large variation in Hf/Nd at almost invariant Nd isotope compositions, therefore,

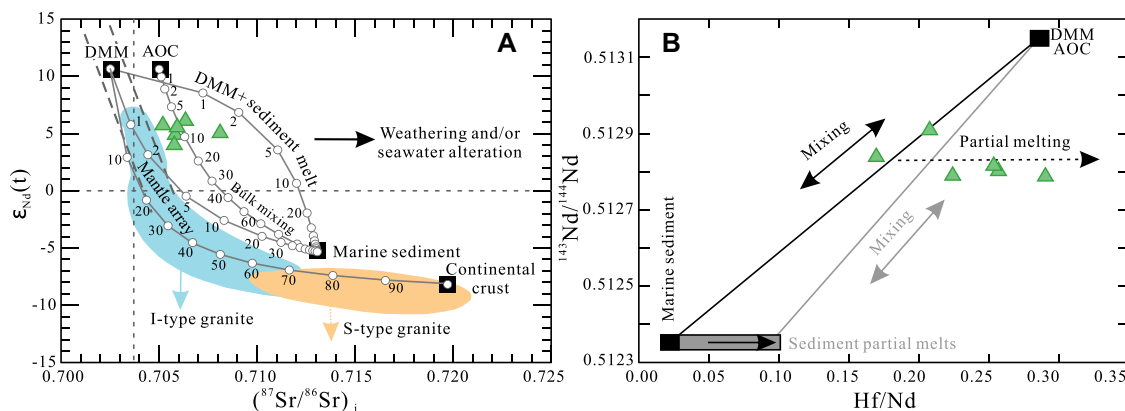


Figure 3. (A) Nd-Sr isotope correlation and mixing modeling results. (B) Nd isotopes versus Hf/Nd ratios. Mixing end members and associated references in A are listed in Table S5 (see footnote 1). Mixing and melting lines in B are modified from Nielsen and Marschall (2017). AOC—altered oceanic crust; DMM—depleted mid-ocean-ridge basalt mantle.

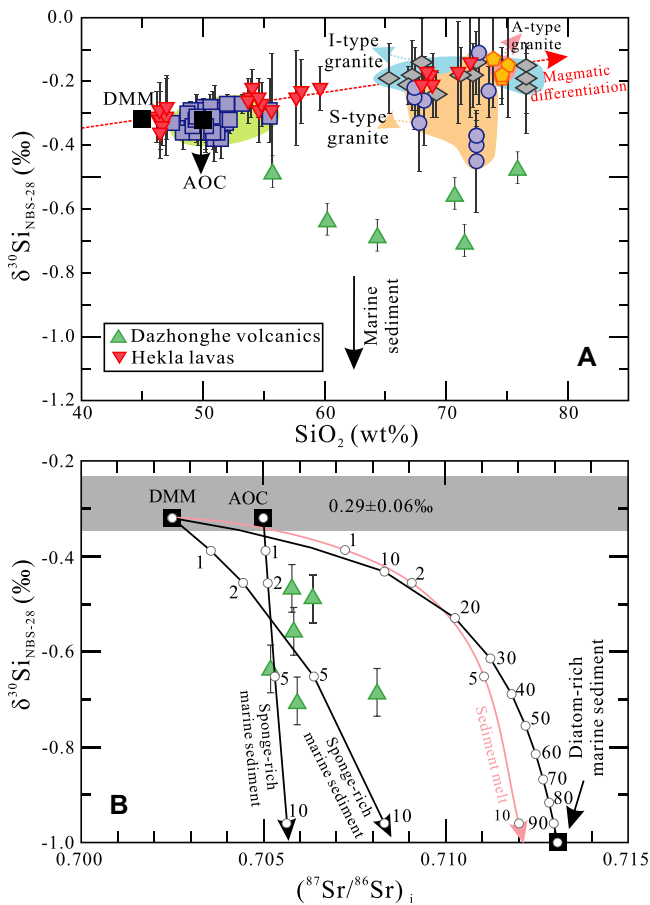


Figure 4. (A) $\delta^{30}\text{Si}_{\text{NBS-28}}$ versus SiO_2 , and (B) $\delta^{30}\text{Si}_{\text{NBS-28}}$ versus $(^{87}\text{Sr}/^{86}\text{Sr})_i$ plots for Dazhonghe arc rocks. Data for altered oceanic crust (AOC), I-type, S-type, and A-type granites, and Hekla (Iceland) lavas (Savage et al., 2011, 2012; Yu et al., 2018) are shown for comparison. Values of mixing end members and associated references are listed in Table S5 (see footnote 1). DMM—depleted mid-ocean-ridge basalt mantle.

suggests that the trace-element fractionation occurred after mixing of the different slab and mantle components, consistent with a mélangé melting scenario (Fig. 3B).

We also carried out mixing calculations of sediment melt and DMM using Sr and Si isotope data (Fig. 4B). The mixing lines again reveal that the Dazhonghe samples plot far away from the sediment melt and DMM mixing lines (Fig. 4B). Thus, the Sr-Nd-Si isotope compositions of the Dazhonghe rocks preclude their derivation from partial melting of a metasomatized mantle wedge and show they were inherited from bulk mixing of subducted sediment, AOC, and depleted mantle.

Si Isotope Evidence

The Si isotopes in mantle-derived rocks are resistant to minor degrees of chemical weathering, mineral dissolution and precipitation, and partial melting (Schauble et al., 2009; Savage et al., 2011). All mantle-derived rocks (including modern arc lavas) exhibit invariant $\delta^{30}\text{Si} = -0.29\text{‰} \pm 0.07\text{‰}$, as shown in Figure 4. Authigenic clay minerals can have light Si isotope compositions (as low as $\delta^{30}\text{Si} -2.3\text{‰}$ for kaolinite), but most show variable $\delta^{30}\text{Si}$ values of -2.3‰ to $+1.8\text{‰}$ (Douthitt, 1982; Trower and Fischer, 2019). Bulk pelagic clay-rich sediments rarely consist exclusively

of authigenic clays, and they have Si isotope compositions rather similar to bulk silicate earth ($\delta^{30}\text{Si} \sim -0.29\text{‰}$; Ehlert et al., 2016; Trower and Fischer, 2019). We assumed the $\delta^{30}\text{Si}$ value for authigenic clays to be -1‰ according to Trower and Fischer (2019) and then did mixing calculations between DMM and authigenic clay minerals as shown in Figure 2. The results revealed that pelagic clay-rich sediments are an unlikely component to account for the observed data. Thus, only Si-bearing marine organisms (e.g., diatoms and marine sponges) preferentially take up the light Si isotopes by up to several per mil, which causes Si-rich marine sediments to display light Si isotope compositions relative to the mantle (Sutton et al., 2013; Stamm et al., 2020). The low $\delta^{30}\text{Si}$ values in the Dazhonghe samples could, therefore, be explained by a subducted sediment component rich in biogenic silica. However, modern Si-rich (diatom-rich) sediments typically display $\delta^{30}\text{Si} > -1\text{‰}$ (Sutton et al., 2013), which would require sediment addition of 20%–30% in order to account for the full range of $\delta^{30}\text{Si}$ values observed in the Dazhonghe samples (Fig. 4B). Such amounts of Si-rich sediment contamination of the mantle wedge in a subduction zone are unrealistic and would produce whole-rock $\delta^{18}\text{O}$, Sr, and Nd isotope compositions very different to those recorded in the lavas (Figs. 2B and 4B).

The Prototethyan ocean existed during the late Neoproterozoic to early Paleozoic, when marine sponges were important parts of the marine ecosystem and probably the dominant Si-bearing component in marine sediments (Li et al., 1998; De La Rocha, 2003). Si isotopic fractionation in marine sponges is much larger than that for diatoms, with $\delta^{30}\text{Si}$ values of marine sponges varying from -6.74‰ to -1.50‰ (Cassarino et al., 2018). Binary mixing calculations using sponge-rich marine sediment and AOC as two end members resulted in mixing lines that reproduced the Dazhonghe $\delta^{30}\text{Si}$ values, while only requiring less than $\sim 5\%$ of sediment addition (Figs. 2 and 4B).

Zircon Hf-O Isotope Evidence

Our mixing calculations using Si-rich marine sediment and AOC, and Si-rich marine sediment and DMM indicated that $\sim 5\%$ sponge-rich marine sediment and $\sim 95\%$ DMM could have produced the Hf-O isotope compositions of the Dazhonghe arc rocks (Fig. 2A), similar to those of the O-Si isotopes. Furthermore, mixing between marine sediments and mantle wedge can also account for the Nd and Hf isotope compositions, as shown in the Figure S5.

CONCLUSIONS

The combined evidence from radiogenic Hf-Nd-Sr isotopes and Si-O stable isotopes revealed that the Paleozoic Dazhonghe continental arc in the southeastern Tibetan Plateau was formed through subduction of marine sponge-rich sediments that formed a mélangé at the slab-mantle interface. The arc lavas likely represent the latest stages of subduction zone volcanism associated with the Prototethyan subduction. The Dazhonghe arc is the first continental arc for which it has been shown that mélangé melting was the driving force for arc magma generation.

ACKNOWLEDGMENTS

H.C. Liu thanks the Science Foundation of China University of Petroleum, Beijing (grant 2462018YJRC030) for financial support. S.G. Nielsen acknowledges support from U.S. National Science Foundation grant EAR-1829546. This manuscript benefited from reviews by Martin Guitreau and an anonymous reviewer, and efficient editorial handling by Gerald Dickens.

REFERENCES CITED

- Bebout, G.E., 2007, Metamorphic chemical geodynamics of subduction zones: Earth and Planetary Science Letters, v. 260, p. 373–393, <https://doi.org/10.1016/j.epsl.2007.05.050>.
- Cassarino, L., Coath, C.D., Xavier, J.R., and Hendry, K.R., 2018, Silicon isotopes of deep sea sponges: New insights into biomineralisation and skeletal structure: Biogeosciences, v. 15, p. 6959–6977, <https://doi.org/10.5194/bg-15-6959-2018>.
- De La Rocha, C.L., 2003, Silicon isotope fractionation by marine sponges and the reconstruction of the silicon isotope composition of ancient deep water: Geology, v. 31, p. 423–426, [https://doi.org/10.1130/0091-7613\(2003\)031<0423:SIFBMS>2.0.CO;2](https://doi.org/10.1130/0091-7613(2003)031<0423:SIFBMS>2.0.CO;2).

- Douthitt, C.B., 1982, The geochemistry of the stable isotopes of silicon: *Geochimica et Cosmochimica Acta*, v. 46, p. 1449–1458, [https://doi.org/10.1016/0016-7037\(82\)90278-2](https://doi.org/10.1016/0016-7037(82)90278-2).
- Ducea, M.N., Saleeby, J.B., and Bergantz, G., 2015, The architecture, chemistry, and evolution of continental magmatic arcs: *Annual Review of Earth and Planetary Sciences*, v. 43, p. 299–331, <https://doi.org/10.1146/annurev-earth-060614-105049>.
- Ehlert, C., Doering, K., Wallmann, K., Scholz, F., Sommer, S., Grasse, P., Geilert, S., and Frank, M., 2016, Stable silicon isotope signatures of marine pore waters—Biogenic opal dissolution versus authigenic clay mineral formation: *Geochimica et Cosmochimica Acta*, v. 191, p. 102–117, <https://doi.org/10.1016/j.gca.2016.07.022>.
- Hermann, J., and Rubatto, D., 2009, Accessory phase control on the trace element signature of sediment melts in subduction zones: *Chemical Geology*, v. 265, p. 512–526, <https://doi.org/10.1016/j.chemgeo.2009.05.018>.
- Kelemen, P.B., and Behn, M.D., 2016, Formation of lower continental crust by relamination of buoyant arc lavas and plutons: *Nature Geoscience*, v. 9, p. 197–205, <https://doi.org/10.1038/ngeo2662>.
- Li, C.W., Chen, J.Y., and Hua, T.E., 1998, Precambrian sponges with cellular structures: *Science*, v. 279, p. 879–882, <https://doi.org/10.1126/science.279.5352.879>.
- Liu, H.C., Bi, M.W., Guo, X.F., Zhou, Y.Z., and Wang, Y.K., 2019, Petrogenesis of late Silurian volcanism in SW Yunnan (China) and implications for the tectonic reconstruction of northern Gondwana: *International Geology Review*, v. 61, p. 1297–1312, <https://doi.org/10.1080/00206814.2018.1506947>.
- Mackie, R.A., Scoates, J.S., Weis, D., Maerschalk, C., and Peck, D., 2005, Trace element and Hf-Nd isotopic profiling of crustal contamination across the marginal zone of the Muskox intrusion, Nunavut: *Geochimica et Cosmochimica Acta*, v. 69, p. A863–A863.
- Marschall, H.R., and Schumacher, J.C., 2012, Arc magmas sourced from mélange diapirs in subduction zones: *Nature Geoscience*, v. 5, p. 862–867, <https://doi.org/10.1038/ngeo1634>.
- Nielsen, S.G., and Marschall, H.R., 2017, Geochemical evidence for mélange melting in global arcs: *Science Advances*, v. 3, p. 1–6, <https://doi.org/10.1126/sciadv.1602402>.
- Pringle, E.A., Moynier, F., Savage, P.S., Jackson, M.G., Moreira, M., and Day, J.M.D., 2016, Silicon isotopes reveal recycled altered oceanic crust in the mantle sources of ocean island basalts: *Geochimica et Cosmochimica Acta*, v. 189, p. 282–295, <https://doi.org/10.1016/j.gca.2016.06.008>.
- Savage, P.S., Georg, R.B., Williams, H.M., Burton, K.W., and Halliday, A.N., 2011, Silicon isotope fractionation during magmatic differentiation: *Geochimica et Cosmochimica Acta*, v. 75, p. 6124–6139, <https://doi.org/10.1016/j.gca.2011.07.043>.
- Savage, P.S., Georg, R.B., Williams, H.M., Turner, S., Halliday, A.N., and Chappell, B.W., 2012, The silicon isotope composition of granites: *Geochimica et Cosmochimica Acta*, v. 92, p. 184–202, <https://doi.org/10.1016/j.gca.2012.06.017>.
- Savage, P.S., Georg, R.B., Williams, H.M., and Halliday, A.N., 2013, The silicon isotope composition of the upper continental crust: *Geochimica et Cosmochimica Acta*, v. 109, p. 384–399, <https://doi.org/10.1016/j.gca.2013.02.004>.
- Savage, P.S., Armytage, R.M.G., Georg, R.B., and Halliday, A.N., 2014, High temperature silicon isotope geochemistry: *Lithos*, v. 190, p. 500–519, <https://doi.org/10.1016/j.lithos.2014.01.003>.
- Schauble, E.A., Young, E.D., Ziegler, K., Shahar, A., Halliday, A.N., and Georg, R.B., 2009, Silicon isotope fractionation at high pressures and temperatures: *Geochimica et Cosmochimica Acta*, v. 73, Supplement 1169, p. A1169–A1169.
- Shu, Y.C., Nielsen, S.G., Le Roux, V., Wörner, G., Blusztajn, J., and Auro, M., 2022, Sources of dehydration fluids underneath the Kamchatka arc: *Nature Communications*, v. 13, p. 4467, <https://doi.org/10.1038/s41467-022-32211-5>.
- Stamm, F.M., Meeheut, M., Zambardi, T., Chmeleff, J., Schott, J., and Oelkers, E.H., 2020, Extreme silicon isotope fractionation due to Si organic complexation: Implications for silica biomineralization: *Earth and Planetary Science Letters*, v. 541, <https://doi.org/10.1016/j.epsl.2020.116287>.
- Sutton, J.N., Varela, D.E., Brzezinski, M.A., and Beucher, C.P., 2013, Species-dependent silicon isotope fractionation by marine diatoms: *Geochimica et Cosmochimica Acta*, v. 104, p. 300–309, <https://doi.org/10.1016/j.gca.2012.10.057>.
- Trower, E.J., and Fischer, W.W., 2019, Precambrian Si isotope mass balance, weathering, and the significance of the authigenic clay silica sink: *Sedimentary Geology*, v. 384, p. 1–11, <https://doi.org/10.1016/j.sedgeo.2019.02.008>.
- Ulmer, P., and Trommsdorff, V., 1995, Serpentine stability to mantle depths and subduction-related magmatism: *Science*, v. 268, p. 858–861, <https://doi.org/10.1126/science.268.5212.858>.
- Valley, J.W., et al., 2005, 4.4 billion years of crustal maturation: Oxygen isotope ratios of magmatic zircon: *Contributions to Mineralogy and Petrology*, v. 150, p. 561–580, <https://doi.org/10.1007/s00410-005-0025-8>.
- Wang, Y.J., Qian, X., Cawood, P.A., Liu, H.C., Feng, Q.L., Zhao, G.C., Zhang, Y.H., He, H.Y., and Zhang, P.Z., 2018, Closure of the East Paleotethyan Ocean and amalgamation of the Eastern Cimmerian and Southeast Asia continental fragments: *Earth-Science Reviews*, v. 186, p. 195–230, <https://doi.org/10.1016/j.earscirev.2017.09.013>.
- Yu, H.M., Li, Y.H., Gao, Y.J., Huang, J., and Huang, F., 2018, Silicon isotopic compositions of altered oceanic crust: Implications for Si isotope heterogeneity in the mantle: *Chemical Geology*, v. 479, p. 1–9, <https://doi.org/10.1016/j.chemgeo.2017.12.013>.

Printed in USA